Planar chiral alkenylferrocene phosphanes: Preparation, structural characterisation and catalytic use in asymmetric allylic alkylation

Petr Štěpnička *, Martin Lamač, Ivana Císařová

Charles University in Prague, Faculty of Science, Department of Inorganic Chemistry, Hlavova 2030, 12840 Prague, Czech Republic

Abstract

Planar chiral alkenylferrocene phosphanes, viz. (S_p)-[Fe(η^5-C$_5$H$_3$-1-PPh$_2$-2-CH=CR$_2$)(η^5-C$_5$H$_5$)] (R = H, (S_p)-**2**; Ph, (S_p)-**5**) and (S_p)-[Fe(η^5-C$_5$H$_3$-1-PPh$_2$-2-(E)-CH=CHR)(η^5-C$_5$H$_5$)] (R = Ph, (S_p)-**3**; C(O)CH$_3$, (S_p)-**6**; and CO$_2$CH$_2$CH$_3$, (S_p)-**7**) have been prepared by alkenylation of (S_p)-2-(diphenylphosphanyl)ferrocenecarboxaldehyde and tested as ligands for enantioselective palladium-catalysed allylic alkylation of 1,3-diphenyprop-2-en-1-yl acetate with dimethyl malonate. All phosphanylalkenes formed active catalysts. However, the induced enantioselectivity was only poor to moderate [12–43% ee after 20 h at room temperature], with the ee's and configuration of the preferred product strongly depending on the ligand structure. The catalytic results have been related to solution properties (NMR, ESI MS) and the solid-state structural data (X-ray diffraction) of [Pd(η^3-1,3-Ph$_2$C$_3$H$_3$){(S_p)-**2**-η^2:κP}]ClO$_4$ ((S_p)-**12**), which represent a model of the plausible reaction intermediate.
© 2007 Elsevier B.V. All rights reserved.

Keywords: Ferrocene; Phosphanes; Alkenes; Alkenylphosphanes; Palladium; Enantioselective allylic alkylation

1. Introduction

Chiral bidentate ferrocene ligands are frequently used as efficient chirality sources to various asymmetric metal-mediated reactions. The most commonly applied ligand families are ferrocene diphosphanes and their monophosphane analogues bearing an additional standard donor moiety, i.e. ligands of the P,P-, P,N-, P,O- and P,S-types [1]. Chiral ferrocene donors that combine a phosphane group with potentially π-coordinating substituent(s) (e.g., C–C double bond) are still very uncommon [2], which contrasts with the current interest in catalytic and coordination chemistry of C-chiral organic phosphanylalkene donors [3,4].

Recently, we have reported about the coordination properties of the achiral ferrocene phosphanylalkene **1**

[5,6] and, shortly afterwards, described also the preparation and coordination behaviour of its planar chiral counterparts (S_p)-**2** and (S_p)-**3** (Scheme 1) [7]. Considering the successful catalytic application of the chiral *organic* alkenylphosphanes [3,4], we decided to extend our studies on chiral alkenylferrocene phosphanes further towards their utilisation in enantioselective catalysis. In view of the coordination ability of alkenylphosphanes (S_p)-**2** and (S_p)-**3** established earlier [7], we chose palladium-catalysed asymmetric allylic alkylation as the testing reaction.

Apart from serving as a benchmark test reaction for chiral ligands, the asymmetric allylic alkylation represents a powerful method for stereoselective construction of new carbon–carbon bonds. With a proper catalyst, it usually proceeds with good yields and enantioselectivity, under mild conditions and, above all, tolerates many reactive functional groups, thus opening an access to *stereodefined* functional allylic products that themselves are valuable synthons [8].

* Corresponding author. Fax: +420 221 951 253.
  E-mail address: stepnic@natur.cuni.cz (P. Štěpnička).
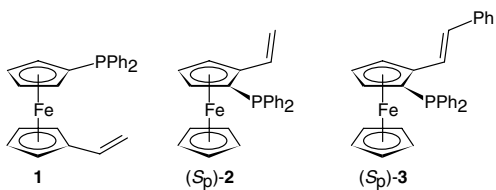
Scheme 1.

Scheme 3.

In this contribution we report about the preparation and catalytic use in palladium-catalysed asymmetric allylic alkylation of a series of planar chiral alkenylferrocene phosphanes formally derived from the archetypal compound (S_p)-2. We also present the solution NMR and solid-state X-ray structural study of complex [Pd(η^3-1,3-Ph$_2$C$_3$H$_3$){(S_p)-2-η^2:κP}]ClO$_4$ ((S_p)-12), which comprises the [Pd(η^3-1,3-Ph$_2$C$_3$H$_3$){(S_p)-2-η^2:κP}]$^+$ cation as the likely reaction intermediate in the alkylation reaction.

2. Results and discussion

2.1. Synthesis and characterisation of the phosphanylalkene ligands

The preparation of (S_p)-2 and (S_p)-3 has been reported elsewhere [7]. Alkenylphosphanes 5–7 were synthesised similarly by Horner–Wadsworth–Emmons alkenylation [9] of enantiomerically pure aldehyde (S_p)-4 [10] with the appropriate phosphonates (Scheme 2). In all cases, the olefination reactions proceeded with excellent yields and gave exclusively the (E)-configured alkenes. The products were conveniently purified by column chromatography and isolated as air stable, intensely coloured solids.

For a comparison, a monodentate, planar-only chiral phosphane with a saturated hydrocarbyl substituent, (S_p)-8, was also prepared. This compound was obtained by diimide reduction [11] of alkene (S_p)-2 (Scheme 3), the
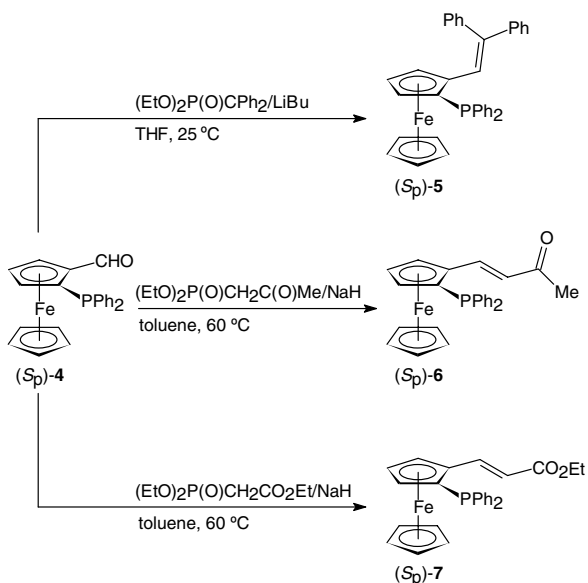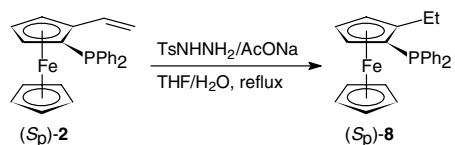
reducing agent being generated in situ from tosyl hydrazine in the presence of sodium acetate in biphasic THF–water mixture at reflux temperature [12].

All newly prepared compounds have been characterised by the conventional spectral methods and their composition confirmed by combustion analysis or high-resolution mass spectra. In ^{1}H and ^{13}C NMR spectra, phosphanes 5–8 show typical sets of signals due to the 1,2-disubstituted ferrocene unit bearing the diphenylphosphanyl group. The presence of α,β-disubstituted alkenyl moieties in (S_p)-6 and (S_p)-7 is reflected by a pair of doublets in ^{1}H NMR spectra that are further split with the phosphorus. As indicated by the $^3J_{HH}$ coupling constants (ca. 16 Hz), the CH=CH double bonds in (S_p)-6 and (S_p)-7 possess the expected (E)-geometry; signals due to the corresponding (Z)-isomers were not detected in the spectra. On the other hand, the spectrum of (S_p)-8 shows a binomial triplet for the terminal methyl group while the diastereotopic methylene protons give rise to a pair of double quartets (ABM$_3$ spin system) with one component showing an additional coupling with the phosphorus (ddq with $^4J_{PH} = 1.6$ Hz).

The ^{13}C NMR resonances of the double bond carbons in (S_p)-6 and (S_p)-7 are observed as phosphorus-coupled doublets with characteristic shifts [$^3J_{PC} = 11$–12 Hz (C$^\alpha$), $^4J_{PC} =$ ca. 2–3 Hz (C$^\beta$)]; the ^{13}C NMR resonance due to CH= in the trisubstituted alkene (S_p)-5 occurs at δ_C 124.31 with $^3J_{PC} = 15$ Hz. By contrast, the ^{31}P NMR signals of 5–8 are rather insensitive to changes within the adjacent alkenyl group, occurring in a narrow range at around δ_P –22.

Phosphanes 5–8 are thermally robust, showing molecular ions in EI mass spectra. Their IR spectra are rather complicated, displaying characteristic bands due to the functional substituents. For instance, the C=O and C=C stretching bands in (S_p)-6 are observed at 1683 and 1599 cm^{-1}, respectively. Whereas the position of the high-energy band corresponds well with that in methyl vinyl ketone, the band due to C=C stretching is shifted to lower energies (by 19 cm^{-1}) because of conjugation with the ferrocene unit [13]. Likewise, the IR bands of (S_p)-7 at 1705 and 1626 cm^{-1} are shifted to lower frequencies than the corresponding bands in ethyl (E)-cinnamate (by ca. 10 and 17 cm^{-1}, respectively) [14].

The phosphanylalkenes are intensely coloured solids, the colour of which changes with the nature of the alkenyl substituent. The vinyl derivative (S_p)-2 and its phenylated analogues (S_p)-3 and (S_p)-5 are rusty brown while compounds (S_p)-6 and (S_p)-7 bearing the conjugated CH=CHC(O) moiety are deep burgundy red. The extent

Scheme 2.
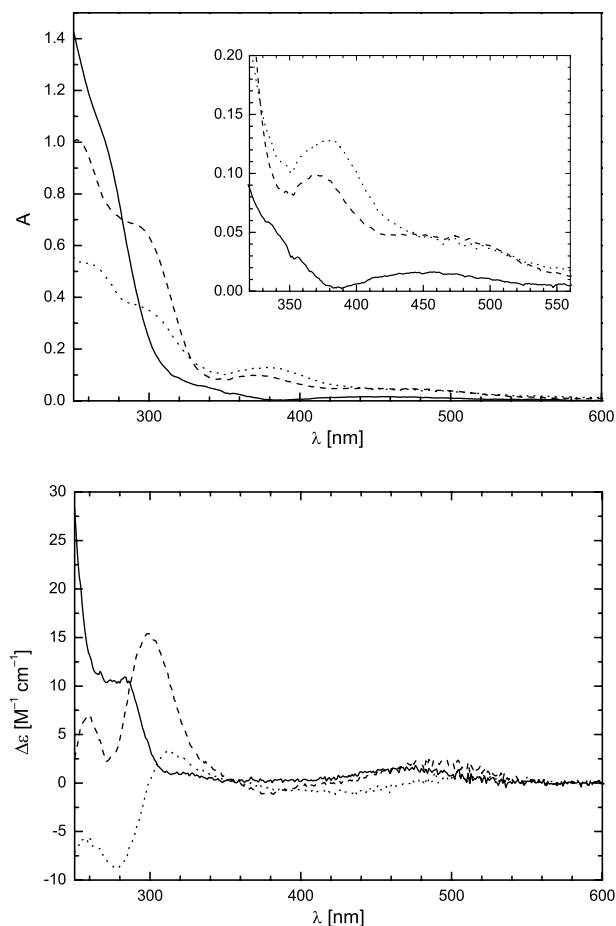
Fig. 1. UV–Vis (top) and CD spectra (bottom) of (S_p)-**2** (solid line), (S_p)-**6** (dashed line), and (S_p)-**7** (dotted line) as recorded on methanol solutions (0.45 mg/mL; optical path 0.5 mm). The inset shows the expansion of the low-energy region of the UV–Vis spectra.

of the π-conjugated chromophore is nicely reflected in UV–Vis spectra (Fig. 1, top). In the visible region, (S_p)-**2** has only a relatively weak, broad band at ca. 460 nm [log(ε/1 M^{-1} cm^{-1}) $\approx$ 2.4]. Compounds (S_p)-**6** and (S_p)-**7** display similar bands at practically identical positions but with a slightly higher intensities. In addition, however, the carbonyl compounds possess additional stronger bands at 378 and 374 nm [log(ε/1 M^{-1} cm^{-1}) = 3.31 and 3.40], respectively, that account for their deep red colour. Further bands occur at higher energies at the slope of much stronger bands extending from the UV region. Their position again varies with the type of the π-system [λ_{max}: (S_p)-**2** ca. 270 nm, (S_p)-**6** and (S_p)-**7** ca. 300 nm].

CD spectra (Fig. 1, bottom) confirm identical configurations at the chirality plane. All compounds show a weak positive Cotton effect at around 460 nm. The CD spectra of the carbonyl derivatives exhibit an additional, positive Cotton band at around 290 nm.

2.2. The crystal structure of (S_p)-6

The structure of (S_p)-**6** has been determined by single-crystal X-ray diffraction. View of the molecular structure

is shown in Fig. 2 and the selected geometric data are given in Table 1. The ferrocene unit in (S_p)-**6** shows a negligible tilt and practically identical Fe-ring centroid distances. Although the ferrocene substituents do not cause any notable torsion to their parent cyclopentadienyl ring as evidenced by the torsion angle τ(C(23)–C(1)–C(2)–P) = 1.8(3)°, they bind somewhat asymmetrically: Whereas the C(2/5)–C(1)–C(23) angles differ by only 2.2°, the difference between the C(1/3)–C(2)–P angles is 5.4°. The phosphanyl group is oriented so that one of its phenyl rings is directed above the ferrocene unit while the other extends away from the alkenyl substituent.

Interatomic distances within the oxobutenyl group compare favourably with those in (E)-4-phenylbut-3-en-2-one [15]. The unsaturated moiety has the expected trans-geometry at the double [torsion angle τ(C(1)–C(23)–C(24)–C(25)) = − 179.7(2)°] and extends away from the phosphanyl
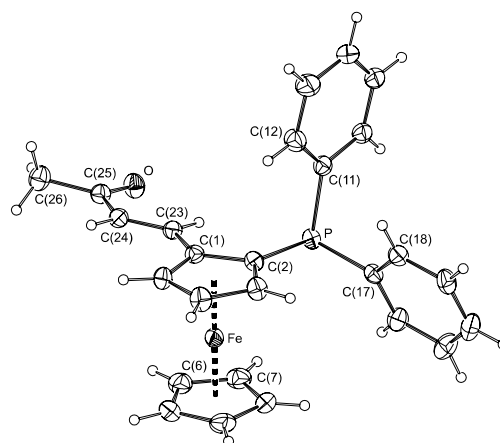
Fig. 2. View of the molecular structure of (S_p)-**6**. Displacement ellipsoids are shown with 30% probability.

Table 1
Selected distances and angles [in Å and °] for (S_p)-**6**[a]

Distances	
Fe–Cg(1)	1.645(1)
Fe–Cg(2)	1.659(1)
P–C(2)	1.818(2)
P–C(11)	1.833(2)
P–C(17)	1.841(2)
C(1)–C(23)	1.448(3)
C(23)–C(24)	1.330(3)
C(24)–C(25)	1.467(3)
C(25)–O	1.219(3)
C(25)–C(26)	1.490(3)
Angles	
∠Cp(1), Cp(2)	0.9(2)
C–P–C[b]	100.2(1)–102.3(1)
C(1)–C(23)–C(24)	126.4(2)
C(23)–C(24)–C(25)	122.2(2)
C(24)–C(25)-O	121.7(2)
C(24)–C(25)–C(26)	117.0(2)

[a] The ring planes are defined as follows: Cp(1) = C(1–5), Cp(2) = C(6–10). Cg(1,2) are the respective ring centroids.
[b] The range of C(2)–P–C(11,C17) and C(11)–P–C(17) angles.

group. Because of conjugation, the C(23)=C(24) double bond is practically coplanar with the Cp(1) ring. The carbonyl carbon atom of the acetyl moiety, C(25), does not deviate from Cp(1) plane either. However, the acetyl group is rotated from the Cp(1) plane by 12.9(3)° along the C(24)–C(25) bond with the C(26) atom being more distant from both the iron centre and the phosphane group [16].

In crystal, the individual molecules of (S_p)-6 associate via C(3)–H(3)···O hydrogen bonds to form infinite helical chains along the 2_1 screw axes parallel to the crystallographic c-axis (space group $P2_12_12_1$; Fig. 3). This interaction appears to be the chief force towards intermolecular aggregation, leading to an antiparallel orientation of the molecular dipoles.

NOESY spectra suggest that the conformation of (S_p)-6 encountered in the solid-state is retained also in solution. The spectrum recorded at 25 °C in CDCl₃ shows NOE correlation for the terminal methyl group at δ_H 2.24 and the CH= group attached to the ferrocene unit (CH$^\alpha$ at δ_H 7.71) and correlation between the =CH$^\beta$ (δ_H 6.38) and the adjacent CH hydrogen of the ferrocene unit (δ_H 4.85). Apparently, the *transoid*-configuration of the C=O and C=C bonds and coplanar disposition of the unsaturated chain and the Cp(1) ring is energetically favoured owing to extensive conjugation of the π-systems.

2.3. Catalytic study

Catalytic ability of 2–8 was probed in palladium-catalysed asymmetric allylic alkylation of racemic 1,3-diphenyl-prop-2-en-1-yl acetate (9) [8], using dimethyl malonate and N,O-bis(trimethylsilyl)acetamide (BSA)/potassium acetate as the nucleophile source [17] and pre-catalysts formed in situ by mixing [{Pd(μ-Cl)(η³-C₃H₅)}₂] with a slight excess of the appropriate ligand (Scheme 4). All reactions were carried out in dichloromethane at room temperature unless noted otherwise. The results are presented in Table 2.

The alkylation reactions proceeded with complete conversions but with only poor to moderate enantioselectivity (entries 1–7 in Table 2). A closer inspection of the data indicates that the ligand structure has a pronounced but
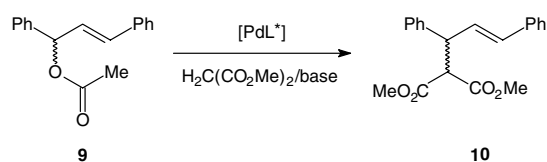
Scheme 4.

rather random influence on the enantioselectivity. This becomes evident even from a comparison of the performance of the simplest ligand (S_p)-2 and its phenylated derivatives (S_p)-3 and (S_p)-5 (entries 1–3). Whereas the catalytic systems based on (S_p)-2 produces predominantly (R)-10, those involving (S_p)-3 and (S_p)-5 give mainly the (S)-configured product, with the ee increasing with bulkiness of the ligand. Similar situation is observed for the ligands bearing the carbonyl substituents (entries 4 and 5). The catalyst resulting from (S_p)-8 afforded 10 enriched with the (R)-enantiomer, similarly to (S_p)-2 albeit with a lower stereodiscrimination. The use two equivalents of (S_p)-8 per palladium did not change the result (entries 6 and 7).

Subsequently, the reaction conditions were optimised for the catalytic system based on (S_p)-2 by surveying alkali metal acetates as the base additive and the reaction temperature (entries 1 and 8–14). The reaction performed with LiOAc afforded the alkylation product with complete conversion but with the lowest enantioselectivity. On the other hand, the reactions carried out in the presence of the heavier alkali metal acetates gave the product with similar ee's but in varying conversions, the reaction rate decreasing with increasing size of the cation. Notably, the reaction performed without the base additive proceeded as well – with very similar ee but only 50% conversion over 20 h (entry 8). Lowering of the reaction temperature had no significant beneficiary effect. Cooling to 0 and −25 °C dramatically reduced the reaction rate while the ee increased only slightly.

2.4. Preparation and structural characterisation of [Pd(η³-1,3-Ph₂C₃H₃){(S_p)-2}]⁺

In order to determine factors controlling the sterochemical course of the alkylation reaction, we studied the cation [Pd(η³-1,3-Ph₂C₃H₃){(S_p)-2}]⁺ as the putative reaction intermediate. Complex [Pd(η³-1,3-Ph₂C₃H₃){(S_p)-2-η²:κP}]ClO₄ ((S_p)-12) was synthesised by cleavage of dimer 11 with the stoichiometric amount of (S_p)-2 followed by treatment with silver(I) perchlorate as a halide scavenger (Scheme 5). Subsequent crystallisation from dichloromethane/acetone–diethyl ether mixture gave CH₂Cl₂-solvated (S_p)-12 as a dark red, microcrystalline solid.

The structure of the complex has been established by single-crystal X-ray diffraction analysis for the solvate (S_p)-12 · CH₂Cl₂. View of the molecular structure is shown in Fig. 4a and the selected geometric data are given in Table 3.
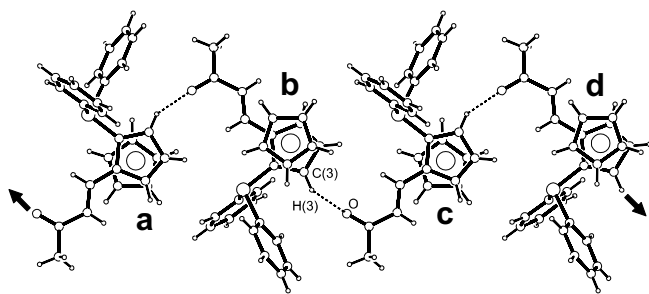
Fig. 3. Section of the hydrogen bonded chains in the structure of (S_p)-6. Selected data: C(3)···O = 3.142(3) Å, angle at H(3) = 124°. Symmetry operations: **a**, 1/2 − x, 1 − y, −1/2 + z; **b**, x, y, z; **c**, 1/2 − x, 1 − y, 1/2 + z; and **d**, x, y, 1 + z.

Table 2
Application of the chiral ligands to palladium-catalysed enantioselective allylic alkylation[a]

Entry	Ligand	T (°C)	Additive	Conversion (%)[b]	ee (%) [config.][c]
1	(Sp)-2	22	KOAc	100 (93)	32 [R]
2	(Sp)-3	22	KOAc	100 (92)	22 [S]
3	(Sp)-5	22	KOAc	100	43 [S]
4	(Sp)-6	22	KOAc	100	26 [S]
5	(R)-7	22	KOAc	100	12 [R]
6	(Sp)-8	22	KOAc	100	18 [R]
7	(Sp)-8[d]	22	KOAc	100	18 [R]
8	(Sp)-2	22	None	50	33 [R]
9	(Sp)-2	22	LiOAc	100	18 [R]
10	(Sp)-2	22	NaOAc	100	29 [R]
11	(Sp)-2	22	RbOAc	90	33 [R]
12	(Sp)-2	22	CsOAc	74	33 [R]
13	(Sp)-2	0	KOAc	58	37 [R]
14	(Sp)-2	−25	KOAc	16	44 [R]

[a] Common details: reaction time 20 h, 5 mol% of Pd-catalyst generated *in situ*. The results are an average of two runs. For detailed conditions, see Section 2.

[b] Conversion determined by ^{1}H NMR spectroscopy. The isolated yields are given in parentheses.

[c] Absolute configuration has been assigned via comparison of the sign of the optical rotation with the literature data [29].

[d] This reaction was performed with two molar equivalents of (Sp)-8 per palladium.

Scheme 5.

phorus lone pair with the ferrocene cyclopentadienyl. Furthermore, the conformation of the ligand changes so as to allow for an efficient chelation. First, the double bond in the complex is rotated above the ferrocene unit, intersecting the least-squares Cp(1) plane at an angle of 40.8(2)° (cf. 7.4(2)° for (Sp)-2). Second, the phosphane group becomes inclined towards the vinyl group. Whereas the C(1/3)–C(2)–P diverge by as much as 12.8°, the vinyl moiety binds to the Cp(1) ring more symmetrically, with the C(2/5)–C(1)–C(23) angles differing only by 3.6°.

The geometry of the Pd((Sp)-2) part is quite regular: the Pd–P and Pd–Cg(3) distances differ by less than 0.08 Å and the P–Pd–Cg(3) angle is by only 3° more acute than the ideal value of 90° (N.B. Cg(3) denotes the geometric centre

Upon going from free (Sp)-2 [7] to the complexed form, there is noted a slight lengthening of the double bond (ca. 0.02 Å). The C(2)–P bond is elongated as well (0.03 Å), presumably due to a diminished conjugation of the phos-
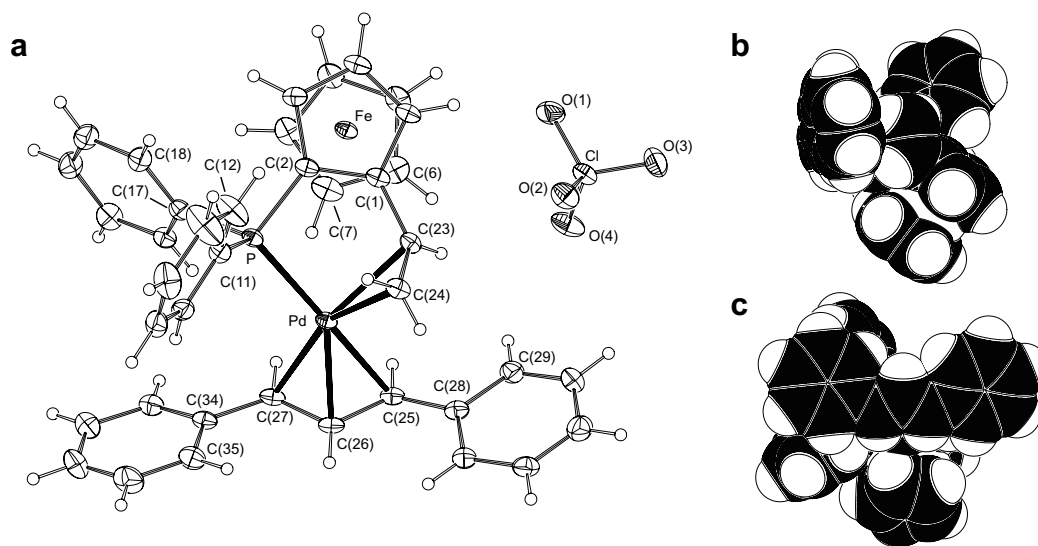
Fig. 4. (a) View of the molecular structure of the complex in the crystals of solvate (Sp)-12 · CH₂Cl₂ showing the atom-labelling scheme. Displacement ellipsoids are drawn with 30% probability. (b,c) Space filling models of the cation in (Sp)-12 as viewed (b) along the C(25)–C(27) line and (c) perpendicular to the plane of the η³-allyl moiety.

Table 3
Selected distances and angles [in Å and °] for (S_p)-12 · CH$_2$Cl$_2^a$

Distances		Angles	
Pd–P	2.3215(9)	P–Pd–Cg(3)	87.04(9)
Pd–Cg(3)	2.245(4)	P–Pd–C(23/24)	84.47(8)/90.01(9)
Pd–C(23)	2.403(3)	Cg(3)–Pd–C(25)	98.0(1)
Pd–C(24)	2.284(4)	Cg(3)–Pd–C(27)	163.4(1)
Pd–C(25)	2.221(3)	P–Pd–C(25)	171.18(7)
Pd–C(26)	2.188(3)	P–Pd–C(27)	109.15(9)
Pd–C(27)	2.199(3)	C(25)–Pd–C(27)	66.4(1)
Fe–Cg(1)	1.640(2)	∠Cp(1), Cp(2)	4.6(2)
Fe–Cg(2)	1.659(2)	C–P–C^c	102.9(2)–108.1(2)
P–C^b	1.786(3)–1.824(3)	C(1)–C(23)–C(24)	123.1(3)
C(23)–C(24)	1.351(4)	C(1)–C(2)–P	119.5(2)
C(1)–C(23)	1.464(4)	C(3)–C(2)–P	132.3(3)
C(25)–C(26)	1.394(5)	C(2)–C(1)–C(23)	124.6(3)
C(26)–C(27)	1.410(5)	C(5)–C(1)–C(23)	128.2(3)

[a] The ring planes are defined as follows: Cp(1) = plane C(1–5), Cp(2) = plane C(6–10). Cg(1, 2) denote the centroids of the cyclopentadienyl ring Cp(1,2) while Cg(3) stands for the midpoint of the C(23)=C(24) double bond.
[b] The range of the P–C(2,11,17) distances.
[c] The range of the C(2)–P–C(11,17) and C(11)–P–C(17) angles.

of the C(23)–C(24) double bond). By contrast, the (η^3-allyl)Pd moiety is considerably twisted. The allyl plane C(25–27) and the plane comprising Pd, P, and Cg(3) intersect each other at an angle of 68.8(3) Å so that the *meso* carbon atom is the most distant from the ferrocene moiety. In accordance with (thermodynamic) *trans*-influence [18], the Pd–C(25) bond *trans* to phosphorus is longer that the Pd–C(27) bond located *trans* to the η^2-coordinated double bond (by 0.022 Å); the shortest, however, being the bond to the *meso* carbon atom C(26). As a consequence of steric demands of the bulky phosphanyl group, the P–Pd–C(26) angle (142.6(1)°) is less acute that the complementary angle Cg(3)–Pd–C(26) (126.0(1)°).

Each complex cation in the crystal interacts with two neighbouring perchlorate ions by means of hydrogen bonds between the H(4) and H(27) and perchlorate oxygens (Fig. 5a). The anions thus act as bridges between cations related by translation along the *b*-axis, which in turn gives rise to infinite alternating chains running parallel to the crystallographic *b*-axis (Fig. 5b).

In solution, complex (S_p)-12 dissociates producing intact cations [Pd(η^3-1,3-Ph$_2$C$_3$H$_3$)(2)]$^+$, that are observed as intense peaks at *m/z* 695 in the ESI+ mass spectra. However, solution NMR spectra revealed the cation in (S_p)-12 to exist as a mixture of isomers differing presumably by conformation of the allyl moiety [19]. The ^{31}P{^{1}H} NMR spectrum recorded at 25 °C displays only very broad, asymmetric signal (Fig. 6). Upon cooling to 0 and −25 °C (Fig. 6), four distinct signals separate that can be tentatively assigned to species involving the isomeric forms of the η^3-allyl moiety (N.B. Only four of the eight possible conformers resulting by exhaustive permutations in the *exo/endo–syn/anti–syn/anti* set were detected) [20]. Unfortunately, a more detailed structural analysis by means of ^{1}H NMR, COSY, and NOESY spectra was not feasible due to extensive overlaps of the signals.
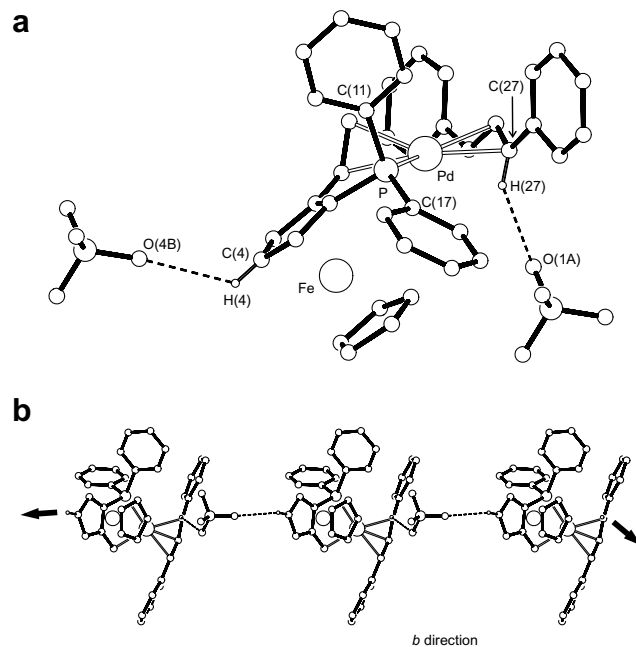
Fig. 5. (a) Hydrogen bonding interactions between the complex cation and the neighbouring perchlorate counter ions in the crystal of (S_p)-12 · CH$_2$Cl$_2$. Geometric data: C(27)–H(27)···O(1A), C(27)···O(1A) = 3.291(4) Å, angle at H(4) = 137°; C(4)–H(4)···O(4B), C(4)···O(4B) = 3.194(4) Å, angle at H(4) = 124°; symmetry operations (A) = 3/2 − x, −1/2 + y, 2 − z; (B) = 3/2 − x, 1/2 + y, 2 − z. Note that the C···O distances are nearly equal to the sum of the van der Waals radii (about 3.2 Å). (b) Section of the infinite hydrogen chains in the crystal of (S_p)-12 · CH$_2$Cl$_2$. The solvent molecules are omitted.

Nonetheless, the collected structural information provides a good base for rationalisation of the catalytic results. The solid-state structure revealed the *exo–syn–syn* geometry for (S_p)-12 which is the obvious precursor to the major product (R)-10 provided that the nucleophilic attack occurs at the site opposite to the donor with relatively stronger *trans* influence (i.e., *trans* to phosphorus; this assumption

a

b
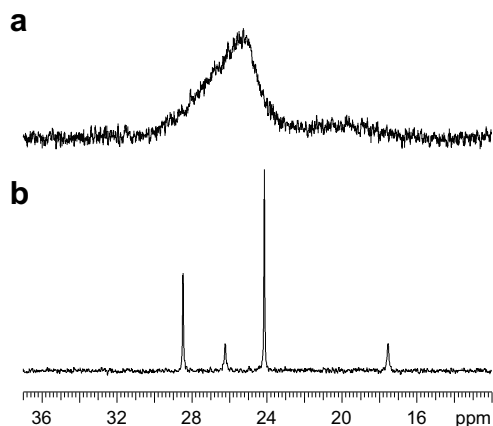
Fig. 6. $^{31}P\{^1H\}$ NMR spectra (161.9 MHz) of (S_p)-**12** recorded in CD_2Cl_2 at (a) 25 and (b) $-25\ ^{\circ}C$. The spectra have been recorded on the same solution but with 24 000 (a) and 280 (b) transitions (exponential weighting was applied to both FIDs; line broadening = 3 Hz).

is supported by Pd–C(25) > Pd–C(27)) [21]. Although any relation between the solution and solid-state data might be considered far reaching, in the present case it is justified by mechanistic studies that indicate the more populated intermediate (i.e., a species thermodynamically preferred in solution and perhaps also in the solid state) to afford the more abundant product enantiomer [22].

Besides, the solid-state structure of (S_p)-**12** accounts for the presence of different reaction intermediates and, hence, only modest enantioselectivity. A plausible explanation can be sought in structural mismatch between the phosphanylalkene ligand and the $Pd(\eta^3\text{-}1,3\text{-}Ph_2C_3H_3)$ moiety. Since the double bond is directly connected to the ferrocene moiety, formation of chelate complexes from **2**–**8** is only possible after rotation of the alkenyl side arm, preferably above the ferrocene unit. The formed donor pocket accommodates the $Pd(\eta^3\text{-}1,3\text{-}Ph_2C_3H_3)^+$ moiety at the side of the ferrocene group so that it sterically interacts with it (see the space filling model in Fig. 4b and c). Consequently, there is no pronounced steric preference for a particular conformation and orientation of the allyl moiety, which in turn results in the observed fluxional behaviour. Since the enantioselectivity is determined by reactivity of the individual allylic species and their exchange rate, the catalysts produce both (S)-**10** and (R)-**10** with only low enantiodiscrimination and varying preference for a single enantiomer. This unfavourable situation can only partly be improved by changing the double bond substituents.

When compared with the analogous catalytic system featuring (1S,4R,7S)-7-(diphenylphosphanyl)-2-phenylnorbornene as the η^2:κP-donor [3a], the ferrocene donors induce lower ee's under similar reaction conditions. The observed difference may be again attributed to steric properties. First, the organic ligand is much less sterically encumbered, which is reflected in the conformer equilibrium (only two isomers in the 56:44 ratio were detected in $CDCl_3$). Second, the spatial arrangement of the donor groups in the organic ligand may better comply with the

steric requirements of the $Pd(\eta^3\text{-allyl})^+$ unit and, above all, provide a much better access for the nucleophile.

3. Summary

A range of planar-only chiral, ferrocene-based alkenylphosphanes can be conveniently accessed via alkenylation of aldehyde (S_p)-**4**. These phosphanylalkene donors readily coordinate to palladium as η^2:κP-chelating donors, forming complexes that are capable of promoting asymmetric allylic alkylation of racemic diphenylallyl acetate (**9**) with dimethyl malonate. The alkylation reactions proceed with complete conversions but only modest enantioselectivity that does not match that of other planar-only chiral bidentate ferrocene ligands [1,8,23]. Based on the solid-state structural data and solution dynamics of complex (S_p)-**12**, which may serve as a model of the anticipated reaction intermediate $[(L\text{–}L')Pd(\eta^3\text{-}PhC_3H_3Ph)]^+$, the limited stereodiscrimination can be accounted for by a structural mismatch within the η^3-allyl intermediate that, in turn, results in its stereochemical non-rigidity and lowers the preference among the reaction intermediates.

4. Experimental

4.1. Materials and methods

All syntheses were performed under an argon atmosphere and with exclusion of the direct daylight. Tetrahydrofuran (THF) was distilled from potassium-benzophenone ketyl. Toluene was dried over sodium or potassium metals and distilled. Dichloromethane was dried over anhydrous potassium carbonate. Compounds (S_p)-**2** and (S_p)-**3** [7], (S_p)-**4** [10], $Ph_2CHP(O)(OEt)_2$ [24], racemic 1,3-diphenylallyl acetate (**9**) [25], and di-μ-chloridobis(η^3-1,3-diphenylallyl)dipalladium(II) (**11**) [26] were synthesised by the literature procedures. Other chemicals and solvents were used as received from commercial sources (Fluka, Aldrich; solvents from Penta).

NMR spectra were measured on a Varian UNITY Inova 400 spectrometer at 25 °C unless noted otherwise. Chemical shifts (δ/ppm) are given relative to internal tetramethylsilane (^1H and ^{13}C) or to an external 85% aqueous H_3PO_4 (^{31}P). The assignment of the NMR signals is based on COSY, NOESY, ^{13}C gHSQC, and ^{13}C gHMBC two-dimensional spectra. IR spectra were recorded on an FT IR Nicolet Magna 760 instrument in the range of 400–4000 cm^{-1}. Mass spectra were obtained on a ZAB-SEQ VG Analytical spectrometer. Electrospray (ESI) mass spectra were recorded with a Bruker Esquire 3000 spectrometer on methanol solutions. CD spectra were obtained with a Jobin Yvon-Spex CD6 spectrometer at room temperature (methanol solutions 0.9 mg/2 mL: $c = 1.14$ mM for (S_p)-**2**, 1.03 mM for (S_p)-**6**, and 0.96 mM for (S_p)-**7**; optical path 0.5 mm). Optical rotations were determined with an automatic polarimeter Autopol III (Rudolph Research) at room temperature.

Safety Note. CAUTION! Although we have not encountered any problems it should be noted that perchlorate salts of metal complexes with organic ligands are potentially explosive and should be handled only in small quantities and with great care.

4.2. Preparation of (S_p)-1-(diphenylphosphanyl)-2-(2,2-diphenylvinyl)ferrocene $[(S_p)$-5]

Butyl lithium (0.8 mL of 2.5 M solution in hexanes, 2.0 mmol) was added to a stirred solution of $Ph_2CHP(O)$-$(OEt)_2$ (760 mg, 2.5 mmol) in dry THF (10 mL) with cooling in an ice bath. After the formed brown solution was stirred at 0 °C for 30 min, a solution of aldehyde (S_p)-4 (399 mg, 1.0 mmol) in THF (10 mL) was added. The cooling bath was removed and the reaction mixture was stirred for 16 h, whereupon its colour changed to bright orange red. The reaction was terminated by addition of brine and the mixture diluted with diethyl ether. The organic layer was separated, washed with brine and dried over $MgSO_4$. Subsequent evaporation afforded crude product as a red orange oil, which was purified by column chromatography (silica gel, hexane–diethyl ether 1:1). The first orange band was collected and evaporated to give (S_p)-5 as an orange brown solid. Yield: 498 mg (91%).

^{1}H NMR (CDCl$_3$): δ 3.61 (dt, 1H, CH of C$_5$H$_3$), 3.70 (dt, 1H, CH of C$_5$H$_3$), 4.04 (s, 5H, C$_5$H$_5$), 4.10 (t, 1H, CH of C$_5$H$_3$), 7.14–7.82 (m, 21H, Ph and =CH). ^{13}C{^{1}H} NMR (CDCl$_3$): δ 70.20 (C$_5$H$_5$), 70.38 (CH of C$_5$H$_3$), 70.60 (d, J_{PC} = 2 Hz, CH of C$_5$H$_3$), 71.61 (d, J_{PC} = 4 Hz, CH of C$_5$H$_3$), 78.10 (d, $^1J_{PC}$ = 7 Hz, C–P of C$_5$H$_3$), 87.48 (d, $^2J_{PC}$ = 10 Hz, C–CH=CPh$_2$ of C$_5$H$_3$), 124.31 (d, $^3J_{PC}$ = 15 Hz, CH=CPh$_2$), 126.81, 126.91 (2C), 127.14, 127.84 (CH of =CPh$_2$); 128.09 (d, J_{PC} = 6 Hz, CH of PPh$_2$), 128.11 (2C, CH of =CPh$_2$), 128.22 (d, J_{PC} = 7 Hz, CH of PPh$_2$), 128.53 (CH of PPh$_2$), 129.11, 130.03 (CH of =CPh$_2$); 130.19 (CH of PPh$_2$), 132.20 (d, J_{PC} = 18 Hz, CH of PPh$_2$), 132.38 (CH of =CPh$_2$), 135.08 (d, J_{PC} = 21 Hz, CH of PPh$_2$), 137.34 (d, $^1J_{PC}$ = 9 Hz, C$_{ipso}$ of PPh$_2$), 139.61 (C$_{ipso}$ of =CPh$_2$ or =CPh$_2$), 139.73 (d, $^1J_{PC}$ = 11 Hz, C$_{ipso}$ of PPh$_2$), 141.13, 142.37 (C$_{ipso}$ of =CPh$_2$ or =CPh$_2$). Note: tentative assignment is given for phenyl carbon atoms due to extensive overlaps in the aromatic region. ^{31}P{^{1}H} NMR (CDCl$_3$): δ –21.6 (s). IR (Nujol): v 1660 (m), 1597 (m), 1317 (m), 1276 (m), 1166 (m), 1106 (m), 1071 (m), 1027 (m), 1000 (m), 940 (m), 918 (m), 817 (s), 763 (s), 742 (vs), 698 (vs), 638 (s), 627 (s), 584 (m), 526 (s), 500 (s), 483 (s), 467 (s), 451 (s) cm^{-1}. MS (EI+): m/z (relative abundance) 548 (2, M$^{+\cdot}$), 364 (9), 340 (8), 182 (28), 105 (100), 77 (85), 51 (39). HR MS calcd. for C$_{36}$H$_{29}$^{56}FeP 548.1356, found 548.1342.

4.3. Preparation of (E,S_p)-1-(diphenylphosphanyl)-2-(3-oxobut-1-en-1-yl)ferrocene $[(S_p)$-6]

An ice-cooled suspension of sodium hydride (92 mg, 3.8 mmol) in dry toluene (20 mL) was treated dropwise with diethyl (2-oxopropyl)phosphonate (1.0 mL, 5.2 mmol) whereupon the solid hydride dissolved with effervescence. After stirring at 0 °C for another 15 min, a solution of (S_p)-4 (798 mg, 2.0 mmol) in warm toluene (20 mL) was added. The resulting mixture was transferred to an oil bath kept at 60 °C and stirred for 18 h (the colour changed from orange to orange red). The reaction was terminated by addition of brine; the organic layer was separated, washed with brine, dried over magnesium sulfate, and evaporated under vacuum. Subsequent purification of the dark red residue by column chromatography (silica gel, hexane–ether 1:2; first red band collected) afforded pure (S_p)-6 as a deep red solid. Yield: 746 mg (85%). The compound can be recrystallised from hot heptane.

^{1}H NMR (CDCl$_3$): δ 2.24 (s, 3H, C(O)CH$_3$), 4.01 (dt, 1H, CH of C$_5$H$_3$), 4.06 (s, 5H, C$_5$H$_5$), 4.58 (t, 1H, CH of C$_5$H$_3$), 4.85 (dt, 1H, CH of C$_5$H$_3$), 6.38 (dd, $^3J_{HH}$ = 16.1, $^5J_{PH}$ = 1.2 Hz, 1H, CH=CHC(O)CH$_3$), 7.08–7.62 (m, 10H, PPh$_2$), 7.71 (dd, $^3J_{HH}$ = 16.1, $^4J_{PH}$ = 2.8 Hz, 1H, CH=CHC(O)CH$_3$). ^{13}C{^{1}H} NMR (CDCl$_3$): δ 26.66 (C(O)CH$_3$), 68.99 (d, J_{PC} = 3 Hz, CH of C$_5$H$_3$), 70.87 (C$_5$H$_5$), 72.39 (CH of C$_5$H$_3$), 74.52 (d, J_{PC} = 4 Hz, CH of C$_5$H$_3$), 79.29 (d, $^1J_{PC}$ = 12 Hz, C–P of C$_5$H$_3$), 83.88 (d, $^2J_{PC}$ = 21 Hz, C–CH=CH of C$_5$H$_3$), 126.01 (d, $^4J_{PC}$ ≈ 2 Hz, CH=CHC(O)CH$_3$), 128.13 (d, J_{PC} = 15 Hz), 128.27, 128.32 (d, J_{PC} = 9 Hz), 129.45, 132.04 (d, J_{PC} = 18 Hz), 135.06 (d, J_{PC} = 21 Hz) (CH of PPh$_2$); 136.58, 139.24 (2× d, $^1J_{PC}$ = 10 Hz, C$_{ipso}$ of PPh$_2$), 143.63 (d, $^3J_{PC}$ = 12 Hz, CH=CHC(O)CH$_3$), 198.20 (C(O)CH$_3$). Note: tentative assignment is given for CH carbons of PPh$_2$ due to extensive overlaps in the region around δ_C 128.2. ^{31}P{^{1}H} NMR (CDCl$_3$): δ –22.8 (s). IR (Nujol): v 1683 (s), 1599 (s), 1260 (m), 1236 (s), 1170 (s), 1106 (m), 1068 (m), 1042 (s), 1000 (s), 976 (s), 915 (s), 743 (s), 830 (s), 808 (s), 751 (vs), 700 (vs), 591 (s), 509 (s), 479 (vs), 464 (s) cm^{-1}. MS (EI+): m/z (relative abundance) 438 (29, M$^{+\cdot}$), 395 (100, [M−COMe]$^+$), 372 (12), 318 (23). HR MS calcd. for C$_{26}$H$_{23}$^{56}FeOP 438.0836, found 438.0839. Anal. Calc. for C$_{26}$H$_{23}$FeOP (438.26): C, 71.25; H, 5.29. Found: C, 70.87; H, 5.27%.

4.4. Preparation of ethyl (E,S_p)-[2-(diphenylphosphanyl)-ferrocenyl]propenoate $[(S_p)$-7]

Triethyl phosphonoacetate (3.0 mL, 15 mmol) was slowly added to an ice-cooled suspension of sodium hydride (0.246 g, 10 mmol) in toluene (15 mL). The hydride dissolved rapidly with copious gas evolution (hydrogen) to give a clear colourless solution. After stirring for 15 min at 0 °C, a solution of (S_p)-4 (2.005 g, 5.0 mmol) in warm toluene (35 mL) was introduced and the reaction vessel was transferred to an oil bath kept at 60 °C. After stirring at this temperature for 16 h (the reaction solution turns from orange to deep orange red), the mixture was quenched by addition of water and diluted with little diethyl ether. The organic layer was separated, washed with brine, dried (MgSO$_4$), and evaporated. The deep red oily residue was

purified by chromatography on silica gel with diethyl ether–hexane (2:1) as the eluent. Collecting the first red band and careful evaporation gave (S_p)-7 as a deep red gummy material, which solidifies upon standing at room temperature. Yield: 2.082 g (89%).

^{1}H NMR (CDCl$_3$): δ 1.29 (t, $^3J_{HH} = 7.2$ Hz, 3H, CH$_2$CH_3), 3.94 (dt, 1H, CH of C$_5$H$_3$), 4.05 (s, 5H, C$_5$H$_5$), 4.18 (q, $^3J_{HH} = 7.2$ Hz, 2H, CH_2CH$_3$), 4.53 (t, 1H, CH of C$_5$H$_3$), 4.82 (dt, 1H, CH of C$_5$H$_3$), 6.12 (d, $^3J_{HH} = 15.7$ Hz, 1 H, CH=CHCO$_2$Et), 7.05–7.62 (m, 10H, PPh$_2$), 7.86 (dd, $^3J_{HH} = 15.7$ Hz, $^4J_{PH} = 2.2$ Hz, 1H, CH=CHCO$_2$Et). ^{13}C{^{1}H} NMR (CDCl$_3$): δ 14.34 (CH$_2$$CH_3$), 60.13 ($CH_2CH_3$), 69.12 (d, $J_{PC} = 3$ Hz, CH of C$_5$H$_3$), 70.77 (C$_5$H$_5$), 72.03 (CH of C$_5$H$_3$), 74.11 (d, $J_{PC} = 4$ Hz, CH of C$_5$H$_3$), 78.87 (d, $^1J_{PC} = 12$ Hz, C–P of C$_5$H$_3$), 84.14 (d, $^2J_{PC} = 22$ Hz, C–CH=CH of C$_5$H$_3$), 116.09 (d, $^4J_{PC} = 3$ Hz, CH=CHCO$_2$Et), 127.88, 128.15 (d, $J_{PC} = 6$ Hz), 128.23 (d, $J_{PC} = 8$ Hz), 129.35, 132.01 (d, $J_{PC} = 18$ Hz), 135.17 (d, $J_{PC} = 21$ Hz) (CH of PPh$_2$); 136.91, 139.91 (2× d, $^1J_{PC} = 10$ Hz, C$_{ipso}$ of PPh$_2$), 143.88 (d, $^3J_{PC} = 11$ Hz, CH=CHCO$_2$Et), 166.98 (CO$_2$Et). ^{31}P{^{1}H} NMR (CDCl$_3$): δ −22.8 (s). IR (Nujol): v 1705 (s), 1626 (s), 1336 (m), 1300 (m), 1262 (m), 1236 (m), 1157 (s), 1039 (m), 846 (m), 821 (s), 742 (vs), 697 (vs), 644 (m), 505 (s), 479 (s) cm^{-1}. MS (EI+): m/z (relative abundance) 468 (91, M$^{+\cdot}$), 439 (84, [M−Et]$^+$), 411 (24), 395 (100, [M−CO$_2$Et]$^+$), 373 (12), 183 (42, [Ph$_2$P−2H]$^+$), 165 (57), 121 (58, [C$_5$H$_5$Fe]$^+$), 56 (34, Fe$^+$). HR MS calcd. for C$_{27}$H$_{25}$^{56}FeO$_2$P 468.0942, found 468.0939.

4.5. Preparation of (S_p)-1-(diphenylphosphanyl)-2-ethylferrocene $[(S_p)$-8$]$

Alkene (S_p)-2 (120 mg, 0.30 mmol) and p-toluenesulfonyl hydrazine (0.560 g, 3.0 mmol) were dissolved in dry THF (15 mL). To the obtained solution was added sodium acetate dissolved in water (0.248 g, 3.0 mmol) and the resulting biphasic mixture was heated at reflux and stirred for 20 h (the colour of the reaction mixture turned gradually from orange to yellow). The reaction was terminated by addition of saturated aqueous K$_2$CO$_3$ solution (15 mL) and stirring for another 1 h. Then, the reaction mixture was diluted with diethyl ether, the organic layer was separated, washed twice with brine, dried (MgSO$_4$) and evaporated. The yellow orange residue was purified by column chromatography (silica gel, hexane–diethyl ether 5:1) to give, after evaporation under vacuum, (S_p)-8 as a yellow gummy residue, which solidifies to a waxy yellow solid. Yield: 98 mg (81%).

^{1}H NMR (CDCl$_3$): δ 1.03 (t, $^3J_{HH} = 7.6$ Hz, 3H, CH$_2$CH_3), 2.38 (dqd, $^2J_{HH} \approx$ $^3J_{HH} \approx 7.5$ Hz, $^4J_{PH} = 1.6$ Hz, 1H, CH_2CH$_3$), 2.54 (dq, $^2J_{HH} \approx$ $^3J_{HH} \approx 7.5$ Hz, 1H, CH_2CH$_3$), 3.63 (dt, 1H, C$_5$H$_3$), 4.02 (s, 5H, C$_5$H$_5$), 4.19 (td, 1H, C$_5$H$_3$), 4.34 (m, C$_5$H$_3$), 7.14–7.56 (m, 10H, PPh$_2$). ^{13}C{^{1}H} NMR (CDCl$_3$): δ 14.84 (s, CH$_2$$CH_3$), 21.46 (d, $^3J_{PC} = 10$ Hz, CH$_2$CH$_3$), 68.44 (CH of C$_5$H$_3$), 69.52 (C$_5$H$_5$), 70.12 (d, $J_{PC} = 4$ Hz, CH of C$_5$H$_3$), 70.55

(d, $J_{PC} = 4$ Hz, CH of C$_5$H$_3$), 74.26 (br s, C–P of C$_5$H$_3$), 96.22 (d, $^2J_{PC} = 24$ Hz, C–Et of C$_5$H$_3$), 128.03 (d, $J_{PC} = 7$ Hz, CH of PPh$_2$), 128.10 (d, $J_{PC} = 7$ Hz, CH of PPh$_2$), 128.14 (d, $J_{PC} \approx 1$ Hz, CH of PPh$_2$), 129.08 (d, $J_{PC} \approx 1$ Hz, CH of PPh$_2$), 132.39 (d, $J_{PC} = 18$ Hz, CH of PPh$_2$), 134.87 (d, $J_{PC} = 20$ Hz, CH of PPh$_2$), 136.98 (d, $^1J_{PC} = 6$ Hz, C$_{ipso}$ of PPh$_2$), 139.25 (d, $^1J_{PC} = 8$ Hz, C$_{ipso}$ of PPh$_2$). ^{31}P{^{1}H} NMR (CDCl$_3$): δ −22.1 (s). IR (Nujol): v 1583 (m), 1306 (m), 1169 (s), 1105 (s), 1087 (m), 1069 (m), 1036 (s), 1001 (s), 836 (m), 827 (s), 814 (s), 743 (s), 698 (s), 572 (m), 497 (s), 483 (s), 455 (s) cm^{-1}. MS (EI+): m/z (relative abundance) 399 (29), 398 (100, M$^{+\cdot}$), 396 (7), 321 (4), 277 (4), 213 (16, [M−PPh$_2$]$^+$), 212 (7), 183 (11, [PPh$_2$−2H]$^+$), 121 (9, [C$_5$H$_5$Fe]$^+$), 56 (4, Fe$^+$). HR MS calcd. for C$_{24}$H$_{23}$^{56}FeP 398.0887, found 398.0876. [α]$_D^{22\ °C}$ −265 (c = 0.5, CHCl$_3$) [27].

4.6. General procedure for allylic alkylation of 9 [28,29]

Ligand (13 μmol) and [{Pd(μ-Cl)(η^3-C$_3$H$_5$)}$_2$] (2.3 mg, 6 μmol) were dissolved in dichloromethane (1 mL). The formed solution was stirred at room temperature for 15 min and then added to a mixture of rac-1,3-diphenylprop-2-en-1-yl acetate (9; 63 mg, 0.25 mmol), the appropriate base (0.025 mmol, see Table 2), and dichloromethane (2 mL). After stirring for another 5 min, N,O-bis(trimethylsilyl)acetamide (BSA; 0.2 mL, 0.8 mmol) and dimethyl malonate (0.1 mL, 0.8 mmol) were successively introduced and stirring was continued at room temperature for 20 h. Then, the reaction mixture was diluted with dichloromethane (5 mL) and washed with saturated aqueous NH$_4$Cl solution (2 × 5 mL). The organic layer was separated, dried over MgSO$_4$ and concentrated under vacuum. Subsequent purification by flash chromatography (silica gel; hexane–ethyl acetate 3:1) afforded the alkylation product (in cases of incomplete conversion as mixtures with unreacted 9).

Enantiomeric excesses were determined from ^{1}H NMR spectra recorded in C$_6$D$_6$ in the presence of chiral lanthanide shift reagent tris(3-trifluoroacetyl-d-camphorato)europium(III), Eu(facam)$_3$ while the configuration of the major component was assigned on the basis of optical rotation of the mixture [30]. The results presented in Table 2 are an average of two independent runs.

4.7. Preparation of $(\eta^3$-1,3-diphenylallyl)$[(S_p)$-1-(diphenylphosphanyl-κP)-2-(η^2-vinyl)ferrocene]-palladium(II) perchlorate $[(S_p)$-12$]$

Complex 11 (33.5 mg, 50 μmol) and (S_p)-2 (40 mg, 0.10 mmol) were dissolved in dichloromethane (2 mL) to give a clear orange solution. The solution was stirred at room temperature for 5 min and treated with a solution of AgClO$_4$ (21 mg, 0.10 mmol) in acetone (1 mL). An off-white (AgCl) precipitate formed immediately while the colour of the reaction mixture turned to deep red. The mixture

was stirred for another 15 min, filtered (PTFE syringe filter, 0.45 μm) and the filtering device washed with dichloromethane (1 mL). The clear filtrate was layered with diethyl ether and the mixture allowed to stand at +4 °C for several days. The separated product was filtered off, washed with diethyl ether and dried under vacuum to give solvated (S_p)-**12** as dark red crystalline solid. Yield: 69 mg.

$^{31}P\{^1H\}$ NMR (CD$_2$Cl$_2$, −25 °C): δ 17.6 (ca. 13%), 24.1 (ca. 48%), 26.2 (ca. 11%), and 28.4 (ca. 28%). $^{31}P\{^1H\}$ NMR (CD$_2$Cl$_2$, 0 °C): δ 18.3, 24.3, 26.3, 28.1 (all broad). IR (Nujol): ν 1553 (m), 1541 (m), 12228 (m), 1168 (m), $ν_3$(ClO$_4$) 1098 (vs, broad); 1027 (m), 1000 (m), 949 (m), 759 (s), 695 (vs), $ν_4$(ClO$_4$) 622 (s); 523 (s), 517 (s), 494 (s), 468 (s), 453 (m) cm^{-1}. MS (ESI+): m/z 695.3 ([Pd(Ph$_2$C$_3$H$_3$)(**2**)]$^+$); the observed isotopic distribution agrees with the calculated one. Anal. Calc. for C$_{39}$H$_{34}$FeClO$_4$PPd · 0.35CH$_2$Cl$_2$ (825.05): C, 57.28; H, 4.24. Found: C, 57.25; H 4.29%.

4.8. X-ray crystallography

Crystals suitable for single-crystal X-ray diffraction analysis were selected directly from the reaction batch $((S_p)$-**12** · CH$_2$Cl$_2$: deep red plate, 0.08 × 0.28 × 0.37 mm^3) or grown by recrystallisation from hot heptane $((S_p)$-**6**: ruby red block, 0.08 × 0.15 × 0.42 mm^3). Full-set diffraction data ($\pm h \pm k \pm l$; $2θ \leqslant 42.0°$ for (S_p)-**6** and

54.2° for (S_p)-**12** · CH$_2$Cl$_2$) were collected on a Nonius KappaCCD diffractometer equipped with a Cryostream Cooler (Oxford Cryosystems) at 150(2) K using graphite monochromatised Mo Kα radiation ($λ = 0.71073$ Å) and analyzed with the HKL program package [31]. The data for (S_p)-**12** · CH$_2$Cl$_2$ were corrected for absorption by using a Gaussian method based on the indexed crystal shape, which is the part of the diffractometer software (the range of transmission factors is given in Table 4).

The structures were solved by direct methods (SIR97 [32]) and refined by full-matrix least-squares routine on F^2 (SHELXL97 [33]). The non-hydrogen atoms were refined with anisotropic displacement parameters while all hydrogens were included in the calculated positions and refined as riding atoms with U_{iso}(H) assigned to a multiple of U_{eq} of their bonding atom. Because the solvate in the structure of (S_p)-**12** · CH$_2$Cl$_2$ is disordered in structural voids, its contribution to the scattering was removed using SQUEEZE routine as incorporated in the PLATON program (two areas of 268 Å^3 and 65 electrons per the unit cell) [34]. Selected crystallographic data are given in Table 4. Geometric parameters and structural drawings were obtained with a recent version of the PLATON program [33]. The calculated numerical values are rounded with respect to their estimated standard deviations (esd's) given with one decimal; parameters involving hydrogen atoms in the calculated positions are given without esd's.

5. Supplementary material

Acknowledgements

Table 4
Crystallographic data, data collection and structure refinement parameters for (S_p)-**6** and (S_p)-**12** · CH$_2$Cl$_2$

Compound	(S_p)-**6**	(S_p)-**12** · CH$_2$Cl$_2$
Formula	C$_{26}$H$_{23}$FeOP	C$_{40}$H$_{36}$Cl$_3$FeO$_4$PPd[a]
M (g mol^{-1})	438.26	880.26
Crystal system	Orthorhombic	Monoclinic
Space group	$P2_12_12_1$ (no. 19)	$C2$ (no. 5)
T (K)	150(2)	150(2)
a (Å)	11.1584(3)	33.4732(9)
b (Å)	11.1584(3)	12.3188(3)
c (Å)	14.4122(3)	9.2526(2)
$β$ (°)		104.074(1)
V (Å^3)	2122.85(9)	3700.8(2)
Z	4	4
$D_{calculated}$ (g mL^{-1})	1.371	1.580
$μ$ (Mo Kα) (mm^{-1})	0.800	1.179
T[b]	_[c]	0.744–0.911
Diffractions total	22728	30943
Unique/observed[d] diffractions	4175/3823	8106/7451
R_{int} (%)[e]	4.5	4.94
R (observed data) (%)[f]	2.90	2.98
R, wR (all data) (%)[f]	3.52, 6.68	3.50, 6.75
Flack's parameter	0.00(1)	–0.01(1)
$Δρ$ (e Å^{-3})	0.39, −0.33	0.40, −0.54

[a] [C$_{36}$H$_{34}$FePPd]ClO$_4$ · CH$_2$Cl$_2$.
[b] The range of transmission coefficients.
[c] Not corrected.
[d] Diffractions with $I_o > 2σ(I_o)$.
[e] $R_{int} = \sum |F_o^2 - F_o^2(\text{mean})| / \sum F_o^2$, where $F_o^2(\text{mean})$ is the average intensity od symmetry-equivalent diffractions.
[f] $R = \sum \|F_o| - |F_c\| / \sum |F_o|$, $wR = [\sum \{w(F_o^2 - F_c^2)^2\} / \sum w(F_o^2)^2]^{1/2}$.

References

[1] Reviews: (a) T. Hayashi, Asymmetric catalysis with chiral ferrocenylphosphine ligands, in: A. Togni, T. Hayashi (Eds.), Ferrocenes: Homogeneous Catalysis, Organic Synthesis, Materials Science, VCH, Weinheim, 1995, pp. 105–142 (Chapter 2);
(b) A. Togni, New chiral ferrocenyl ligands for asymmetric catalysis, in: A. Togni, R.L. Halterman (Eds.), Metallocenes, vol. 2, Wiley-VCH, Weinheim, 1998, pp. 685–721 (Chapter 11);
(c) R.G. Arrayás, A. Adrio, J.C. Carretero, Angew. Chem. Int. Ed. 45 (2006) 7674;
(d) P. Barbaro, C. Bianchini, G. Giambastiani, S.L. Parisel, Coord. Chem. Rev. 248 (2004) 2131;
(e) T.J. Colacot, Chem. Rev. 103 (2003) 3101;

(f) H.-U. Blaser, W. Brieden, B. Pugin, F. Spindler, M. Studer, A. Togni, Top. Catal. 19 (2002) 3.

[2] During the course of our work, Stemmler and Bolm reported the preparation of 1-(diphenylphosphanyl)-2-alkenylferrocenes and their 1,1′-isomers (alkenyl = cyclohex-1-en-1-yl, 1,7,7-trimethylbicyclo[2.2.1]hept-2-en-2-yl, and 3-methyl-6-(1-methylethyl)-cyclohex-1-en-1-yl) and tested these donors in conjugate addition of phenylboronic acid to cyclohexenone: R.T. Stemmler, C. Bolm, Synlett (2007) 1365.

[3] Chiral 7-(diphenylphosphanyl)-2-R-norbornenes (R = Ph, benzyl, 3,5-dimethylphenyl) and 7-PR$_2$-2-phenylnorbornenes (PR$_2$ = P(C$_6$H$_4$OMe-4)$_2$, P(C$_6$H$_4$CF$_3$-4)$_2$, and 9-phosphafluoren-9-yl): (a) R. Shintani, W.-L. Duan, K. Okamoto, T. Hayashi, Tetrahedron Lett. 16 (2005) 3400;
(b) R. Shintani, W.-L. Duan, T. Nagano, A. Okada, T. Hayashi, Angew. Chem. Int. Ed. 44 (2005) 4611;
(c) W.-L. Duan, H. Iwamura, R. Shintani, T. Hayashi, J. Am. Chem. Soc. 129 (2007) 2130.

[4] (5H-Dibenzo[a,d]cyclohepten-5-yl)diphenylphosphane and its substitution derivatives: (a) P. Marie, S. Deblon, F. Breher, J. Geier, C. Böhler, H. Rüegger, H. Schönberg, H. Grützmacher, Chem. Eur. J. 10 (2004) 4198;
(b) E. Piras, F. Läng, H. Rüegger, D. Stein, M. Wörle, H. Grützmacher, Chem. Eur. J. 12 (2006) 5849.

[5] P. Štěpnička, I. Císařová, Collect. Czech. Chem. Commun. 71 (2006) 215.

[6] Compound 1 has been previously reported as by-product arising from acid-catalysed dehydration of 1-(diphenylphosphanyl)-1′-(1-hydroxyethyl)ferrocene and used in reactions with [(Cy$_3$P)$_2$Cl$_2$Ru=CHPh] (Cy = cyclohexyl). (a) I.R. Butler, W.R. Cullen, Can. J. Chem. 61 (1983) 147;
(b) I.R. Butler, S.J. Coles, M.B. Hursthouse, D.J. Roberts, N. Fujimoto, Inorg. Chem. Commun. 6 (2003) 760.

[7] P. Štěpnička, I. Císařová, Inorg. Chem. 45 (2006) 8785.

[8] (a) B.M. Trost, D.L. Van Vranken, Chem. Rev. 96 (1996) 395;
(b) B.M. Trost, M.L. Crawley, Chem. Rev. 103 (2003) 2921;
(c) B.M. Trost, J. Org. Chem. 69 (2004) 5813;
(d) T. Hayashi, Asymmetric allylic substitution and Grignard cross-coupling, in: I. Ojima (Ed.), Catalytic Asymmetric Synthesis, VCH, New York, 1993, pp. 325–365 (Chapter 7.1);
(e) T. Graening, H.-G. Schmalz, Angew. Chem. Int. Ed. 42 (2003) 2580;
(f) G. Helmchen, J. Organomet. Chem. 576 (1999) 203;
(g) G. Consiglio, R.M. Waymouth, Chem. Rev. 89 (1989) 257.

[9] (a) B.E. Maryanoff, A.B. Reitz, Chem. Rev. 89 (1989) 863;
(b) W.S. Wadsworth Jr., Org. React. 25 (1977) 73.

[10] (a) O. Riant, O. Samuel, H.B. Kagan, J. Am. Chem. Soc. 115 (1993) 5835;
(b) O. Riant, O. Samuel, T. Flessner, S. Taudien, H.B. Kagan, J. Org. Chem. 62 (1997) 6733.

[11] (a) D.J. Pasto, R.T. Taylor, Org. React. 40 (1991) 91;
(b) S. Hüning, H.R. Müller, W. Thier, Angew. Chem. 77 (1965) 368.

[12] Enantiomer (R$_p$)-8 has been previously obtained by another route: T. Hayashi, T. Mise, M. Fukushima, M. Kagotani, N. Nagashima, Y. Hamada, A. Matsumoto, S. Kawakami, M. Konishi, K. Yamamoto, M. Kumada, Bull. Chem. Soc. Japan 53 (1980) 1138.

[13] R. Mecke, K. Noack, Chem. Ber. 93 (1960) 210.

[14] E. Dallwigk, E. Briner, Helv. Chim. Acta 37 (1954) 620.

[15] A. Degen, M. Bolte, Acta Crystallogr., Sect. C, Crystal. Struct. Commun. 55 (1999) IUC990170 (CIF access article).

[16] Dihedral angle subtended by the C(23)=C(34) vector and the Cp(1) plane is 5.9(2)° while the distances from the Cp(1) plane are: 0.059(2) Å for C(23), 0.077(2) Å for C(24), 0.009(2) Å for C(25), 0.260(2) Å for O, and 0.259(3) Å for C(26).

[17] (a) B.M. Trost, D.J. Murphy, Organometallics 4 (1985) 1143;
(b) M.T. El Gihani, H. Heaney, Synthesis (1998) 357.

[18] (a) T.G. Appleton, H.C. Clark, L.E. Manzer, Coord. Chem. Rev. 10 (1973) 335;

(b) F.R. Hartley, The Chemistry of Platinum and Palladium, Applied Science, London, 1973, pp. 299–303.

[19] Selected examples of NMR studies on (η^3-allyl)palladium complexes with planar chiral, bidentate ferrocene ligands: (a) P.S. Pregosin, R. Salzmann, A. Togni, Organometallics 14 (1995) 842;
(b) P. Barbaro, P.S. Pregosin, R. Salzmann, A. Albinati, R.W. Kunz, Organometallics 14 (1995) 5160;
(c) U. Burckhardt, V. Gramlich, P. Hofmann, R. Nesper, P.S. Pregosin, R. Salzmann, A. Togni, Organometallics 15 (1996) 3496;
(d) R. Fernández-Galán, F.A. Jalón, B.R. Manzano, J. Rodíguez-de la Fuente, M. Vrahami, B. Jedlicka, W. Weissensteiner, G. Jogl, Organometallics 16 (1997) 3758;
(e) F. Gómez-de la Torre, F.A. Jalón, A. López-Agenjo, B.R. Manzano, A. Rodríguez, T. Sturm, W. Weissensteiner, M. Martínez-Ripoll, Organometallics 17 (1998) 4634;
(f) T. Tu, Y.-G. Zhou, X.L. Hou, L.-X. Dai, X.-C. Dong, Y.-H. Yu, J. Sun, Organometallics 22 (2003) 1255;
(g) C.-W. Cho, J.-H. Son, K.H. Ahn, Tetrahedron: Asymmetry 17 (2006) 2240.

[20] Prefixes syn and anti specify the position of the terminal phenyl rings with respect to the central allylic CH group (meso). Conformers are denoted as exo(endo) when the meso-CH group is directed away from (towards) the ferrocene unit.

[21] Theoretical studies: (a) P. Bloechl, A. Togni, Organometallics 15 (1996) 4125;
(b) T.R. Ward, Organometallics 15 (1996) 2836.

[22] The mechanistic study by Bosnich et al. has shown the major allylic intermediate to produce the major product enantiomer: P.B. Mackenzie, J. Whelan, B. Bosnich, J. Am. Chem. Soc. 107 (1985) 2046.

[23] For recent examples, see: M. Lamač, J. Tauchman, I. Císařová, P. Štěpnička, Organometallics 27 (2007) 5042;
(b) J.H. Lee, S.U. Son, Y.K. Chung, Tetrahedron: Asymmetry 14 (2003) 2109;
(c) O.G. Mancheño, J. Priego, S. Cabrera, R.G. Arrayás, T. Llamas, J.C. Caretero, J. Org. Chem. 68 (2003) 3679.

[24] C. Ha, J.H. Horner, M. Newcomb, T.R. Varick, B.R. Arnold, J. Lusztyk, J. Org. Chem. 58 (1993) 1194.

[25] Acetate 9 was prepared by acetylation of 1,3-diphenylallyl alcohol, which results from reduction of chalcone: (a) E.P. Kohler, H.M. Chadwell, Org. Synth. Coll. 1 (1941) 78;
(b) W. Leung, S. Cosway, R.H.V. Jonmes, H. McCann, M. Wills, J. Chem. Soc., Perkin Trans. 1 (2001) 2588;
(c) I.D.G. Watson, S.A. Styler, A.K. Yudin, J. Am. Chem. Soc. 126 (2004) 5086.

[26] T. Hayashi, A. Yamamoto, Y. Ito, E. Nishioka, H. Miura, K. Yanagi, J. Am. Chem. Soc. 111 (1989) 6301.

[27] The (R$_p$)-enantiomer was reported to have [α]$_D^{25\,°C}$ = +273 (c = 0.3, CHCl$_3$). See Ref. [12].

[28] W. Zang, Y. Yoneda, T. Kida, Y. Nakatsuji, I. Ikeda, Tetrahedron: Asymmetry 9 (1998) 3371.

[29] D. Drahoňovský, I. Císařová, P. Štěpnička, H. Dvořáková, P. Maloň, D. Dvořák, Collect. Czech. Chem. Commun. 66 (2001) 588.

[30] T. Hayashi, A. Yamamoto, T. Hagihara, Y. Ito, Tetrahedron Lett. 27 (1986) 191.

[31] Z. Otwinowski, W. Minor, HKL Denzo and Scalepack Program Package, Nonius BV, Delft, The Netherlands;
For a reference, see: Z. Otwinowski, W. Minor, Methods Enzymol. 276 (1997) 307.

[32] A. Altomare, M.C. Burla, M. Camalli, G.L. Cascarano, C. Giacovazzo, A. Guagliardi, A.G.G. Moliterni, G. Polidori, R. Spagna, J. Appl. Crystallogr. 32 (1999) 115.

[33] G.M. Sheldrick, SHELXL97. Program for Crystal Structure Refinement from Diffraction Data, University of Gottingen, Germany, 1997.

[34] A.L. Spek, PLATON—a multipurpose crystallographic tool, Utrecht University, Utrecht, The Netherlands, 2003 and updates. Available at http://www.cryst.chem.uu.nl/platon/.